

SYNTHESIS, CHARACTERIZATION AND PHOTOCATALYTIC ACTIVITY OF NOVEL MIXED METAL OXIDES/REDUCED GRAPHENE OXIDE HYBRID CATALYSTS

Dang Nguyen Nha Khanh¹, Nguyen Thi Mai Tho³, Nguyen Quoc Thang³,
Nguyen Thanh Tien¹, Chau Tan Phong⁴, Mai Huynh Cang⁴,
Nguyen Thi Kim Phuong^{1, 2, *}

¹Hochiminh city Institute of Resources Geography,
Vietnam Academy of Science and Technology, 01 Mac Dinh Chi, District 1, Ho Chi Minh City

²Graduate University of Science and Technology, Vietnam Academy of Science and Technology,
18 Hoang Quoc Viet, Cau Giay, Ha Noi

³Chemical Engineering Faculty, Industrial University of Ho Chi Minh City, Ho Chi Minh City

⁴Nong Lam University Ho Chi Minh City

*Email: nguyenthikimp@yahoo.ca

Received: 11 March 2019; Accepted for publication: 16 July 2019

Abstract. A novel series of ZnBi₂O₄/rGO hybrid catalysts were synthesized via co-precipitation method. The as-prepared catalysts were characterized by X-ray diffraction, Fourier transform infrared, UV-vis diffuse reflectance spectra, Field-emission scanning electron microscopy and Transmission electron microscopy techniques. The photocatalytic activities of ZnBi₂O₄/rGO catalysts were conducted using Indigo Carmine and the ZnBi₂O₄/rGO offered better degradation of pollutants as compared to pristine ZnBi₂O₄. Among them, ZnBi₂O₄/rGO (rGO = 2 %) owned the best photocatalytic activity, which can degrade more than 91 % of Indigo Carmine (50 mg/L) after 75 min visible light irradiation. The enhancement of photocatalytic properties of ZnBi₂O₄/rGO indicates that the existence of rGO may have facilitated photoinduced electrons to move from ZnBi₂O₄ to rGO, which effectively cause separation of the photoinduced electron-hole pairs in ZnBi₂O₄. The ZnBi₂O₄/rGO can be considered as a promising photocatalyst for dye waste water treatment.

Keywords: ZnBi₂O₄/rGO hybrid catalysts; Indigo Carmine; visible-light irradiation, photodegradation.

Classification numbers: 2.6.1, 2.4.2, 2.4.4.

1. INTRODUCTION

In recent years, organic dyes in waste water have become one of the main pollutants in our daily lives. However, these organic dyes have high stability and durability, conventional treatment technologies (physical, chemical and biological) cannot completely eliminate dyes in

solution. To solve this problem, advanced oxidation processes (AOP) including photo-Fenton oxidation, heterogeneous photocatalysis and electrocatalytic oxidation are being extensively studied [1-3]. Photocatalysis involves the excitation of semiconductor materials by light absorption to produce electron-hole pairs, following charge-pair separation to induce the oxidation of organic pollutants [4]. To date, semiconducting photocatalysts such as ZnBi_2O_4 , Bi_2WO_6 , Bi_2O_3 , $\text{Bi}_2\text{Sn}_2\text{O}_7$, $\gamma\text{-Bi}_2\text{MoO}_6$, $\text{Sm}_2\text{FeTaO}_7$, ZnFe_2O_4 have been proved to be promising materials to degrade the organic pollutants in waste water [4-9].

ZnBi_2O_4 is considered as the one of the best semiconductor photocatalyst due to its non-toxicity, narrow band gap, good stability and excellent photocatalytic activity. Recently, numerous research groups have investigated the effectiveness of ZnBi_2O_4 photocatalyst to eliminate organic pollutants under visible light irradiation [4,10,11]. Graphene has a perfect sp^2 hybridized two dimensional carbon structure with excellent conductivity and large surface area [12], so that graphene owns excellent electron conductivity and high adsorption [13]. Hence, graphene-modified semiconductor nanocomposites were regarded as novel photocatalysts for degradation of pollutants.

In recent years, the coupling of two or more different semiconductors with suitable band edge potential has become the most effective approach to improve the photocatalytic performance of semiconductor photocatalysts. Compared with single-component semiconductors, coupling structures are beneficial to promote photocatalytic activity because of improved visible light absorption, increased charge transfer, and enhanced separation of photogenerated electron-hole pairs [4,8]. Although recent advances have been established according to the approaches mentioned above, practical applications are still unsatisfactory. Therefore, it is still a challenge to develop new strategies to build new heterogeneous semiconductor photocatalysts.

This work focused on combining the superior qualities of the functionalized ZnBi_2O_4 with rGO to fabricate $\text{ZnBi}_2\text{O}_4/\text{rGO}$ hybrid catalysts. The photocatalytic activities of the as-synthesized samples for the Indigo carmine degradation were investigated and discussed.

2. MATERIALS AND METHODS

2.1. Materials

All chemicals used were of analytical grade. Graphite, sulfuric acid (H_2SO_4), nitric acid (HNO_3), hydrogen peroxide (H_2O_2), potassium permanganate (KMnO_4), sodium nitrate (NaNO_3), sodium borohydride (NaBH_4), zinc (II) nitrate hexahydrate ($\text{Zn}(\text{NO}_3)_2 \cdot 6\text{H}_2\text{O}$), and Indigo carmine used for this study were purchased from Sigma-Aldrich. Bismuth (III) nitrate pentahydrate ($\text{Bi}(\text{NO}_3)_3 \cdot 5\text{H}_2\text{O}$) and sodium hydroxide (NaOH) were obtained from Junsei Chemical Co., Japan.

2.2. Equipment

The crystalline phases of samples were investigated using a Rigaku Ultima IV X-ray diffractometer (Japan). The measurements were carried out at room temperature with $\text{Cu K}\alpha$ radiation ($\lambda = 1.54051\text{\AA}$) at 40 kV and 40 mA, and diffractograms were recorded in the region of 2θ from 10° to 50° . Transmission electron microscopy (TEM) analyses were conducted with the use of a JEM 1400 microscope. Scanning electron microscopy (SEM) was performed using an S-4800 field emission SEM (FESEM, Hitachi, Japan). Solid state UV-Vis diffuse reflectance

spectra (DRS) were recorded on a Jasco V 550 UV-Vis spectrophotometer (Japan). Fourier transform infrared spectroscopy was recorded by Perkin Elmer FTIR Spectrophotometer RXI (U.S). Photocurrent measurements were performed using a potentiostat (IviumStat, Netherland). The liquid TOC of samples was performed using Shimadzu TOC-VCPH analyzer (Japan). The concentration of Indigo carmine was determined with a Thermo Evolution 201 UV-Visible spectrophotometer (U.S.) over the range of 800 to 200 nm using quartz cuvettes.

2.3. Synthesis

2.3.1. Preparation of reduced graphene oxide (rGO)

Graphene oxide (GO) was prepared using chemical oxidation method [11, 14] with the starting material graphite and for that the mixture of graphite and NaNO_3 was slowly added to 98 % H_2SO_4 under stirring in ice bath for 3 h. KMnO_4 was gradually added to the above suspension and stirred continually under an ice bath to maintain the reaction temperature below 20 °C. Then, the reaction mixture was stirred at 35°C for 2 h to form a thick paste. Subsequently, distilled water was slowly added to the formed paste, followed by another 2 h stirring at 98 °C. After that, for stopping the oxidation reaction more distilled water was added. Sequentially, 30 % H_2O_2 was added into the above mixture and yellow color appeared. The obtained graphite oxide was washed with 5 % HCl, then with distilled water until pH 7. After that, graphite oxide was dispersed in distilled water and exfoliated to generate GO sheets through ultrasonic treatment in 4 h. Finally, GO sheets were collected by centrifugation for 20 minutes at 4000 rpm and dried in a vacuum oven at 80 °C for 24 hours.

Reduced graphene oxide (rGO) was prepared by reducing GO with NaBH_4 . To obtain rGO, the GO was dispersed into distilled water, followed by addition of NaBH_4 to reduce the carboxyl groups and oxygen functional groups. The mixture was then refluxed for 24 h at 100 °C. Finally, the rGO sample was washed with distilled water until the pH became 7 and dried in a vacuum oven at 80 °C for 24 h.

2.3.2. Preparation of ZnBi_2O_4 /reduced graphene oxide (ZnBi_2O_4 /rGO) hybrid materials

For the preparation of $\text{rGO}/\text{ZnBi}_2\text{O}_4$ hybrid materials, the obtained rGO with different proportions ($x = 0, 1, 2$ and 3 %) were evenly dispersed in distilled water by ultrasonication for 30 min at 75 ± 5 °C. A solution of $\text{Zn}(\text{NO}_3)_2 \cdot 6\text{H}_2\text{O}$ and $\text{Bi}(\text{NO}_3)_3 \cdot 5\text{H}_2\text{O}$ in nitric acid (5 %) with molar ratio of 3:1 and an alkaline solution of 1 M NaOH were added dropwise to rGO solutions (flow rate of 2 mL min^{-1}). The pH value of the mixture solutions was maintained around 10. The mixture was stirred continuously for 24 h at 75 ± 5 °C. The precipitate was then collected by centrifugation, washed with distilled water and dried at 70 °C for 10 h, followed by annealing at 450 °C for 3 h to obtain the ZnBi_2O_4 /rGO hybrid materials. The obtained ZnBi_2O_4 /rGO hybrid materials were labeled as ZnBi_2O_4 , $\text{ZnBi}_2\text{O}_4/1.0\text{rGO}$, $\text{ZnBi}_2\text{O}_4/2.0\text{rGO}$ and $\text{ZnBi}_2\text{O}_4/3.0\text{rGO}$ corresponding to 0, 1, 2 and 3 % of rGO in hybrid materials.

2.4. Photocatalytic experiment

Photodegradation of Indigo carmine was carried out in a hollow cylindrical glass batch photoreactor with a working capacity of 100 mL and equipped with a water jacket used in this study. Cooling water from a Refrigerated Circulating Baths (PolyScience, USA) was circulated through the photoreactor jacket to keep the temperature at 30 °C. A 300 W halogen bulb

(luminous flux = 8100 Lm) (Osram 64514, Germany) with full spectrum emission without using filter was employed for visible-light irradiation. The halogen bulb was placed in a protective quartz tube. The quartz tube was immersed in the solution and located in the center of the photoreactor. The reaction solution was agitated with a magnetic stirrer (500 rpm) to keep the catalyst suspended. The photoreactor was covered with aluminium foil to prevent contact with external light. The photocatalytic experiments were performed in closed reactor to avoid solution evaporation. For all experiments, 100 mg of each catalyst was suspended in a 100 mL solution containing 50 mg.L⁻¹ of Indigo carmine at pH ~ 6.3. Before irradiation, the solution of Indigo carmine and the catalyst were stirred in a dark room for 30 min to establish the adsorption/desorption equilibrium between Indigo carmine and the catalyst surface and then the halogen bulb was turned on. The reactions were carried out in triplicate, and 5 mL aliquots were sampled at different time intervals (up to 75 min) then immediately filtered to remove the catalyst. The quantity of Indigo carmine in solution was determined by measuring the UV-Vis absorption. Doubly distilled water was used throughout this study.

3. RESULTS AND DISCUSSION

3.1. Characterization of materials

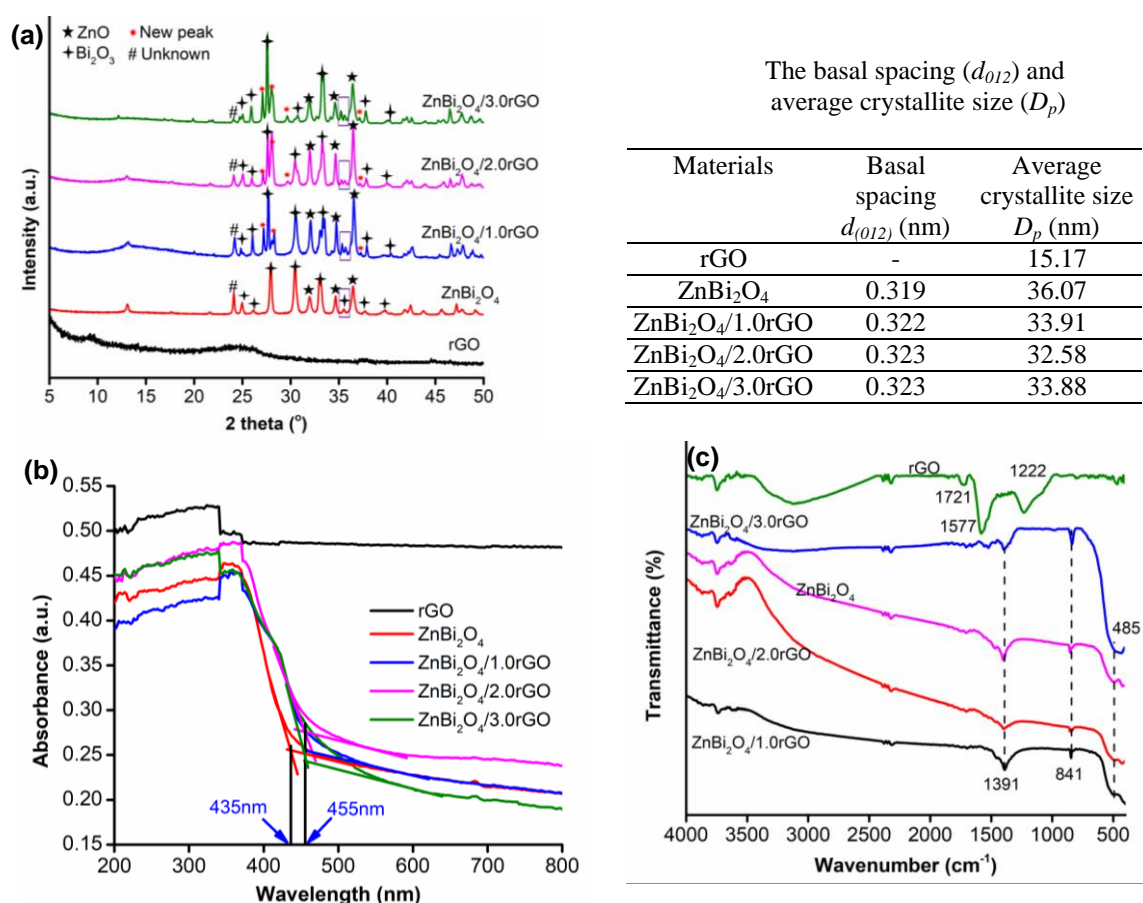


Figure 1. (a) XRD pattern; (b) DRS plot and (c) FT-IR spectra of as-prepared samples.

The XRD pattern of pristine rGO, pristine ZnBi_2O_4 and $\text{ZnBi}_2\text{O}_4/\text{rGO}$ samples are shown in Figure 1a. The XRD pattern of the rGO showed a weak and broad diffraction peak at 2θ value 24.6° that could be assigned to the diffractions of the (002) plane [11]. This indicated that the carboxyl groups and oxygen function groups are completely reduced on rGO sample [15]. All of the diffraction peaks of pristine ZnBi_2O_4 could be indexed to the ZnO and Bi_2O_3 . The sharp peaks located at 31.98 , 34.66 and 36.47° can be unambiguously indexed to (100), (002) and (101) planes of hexagonal ZnO (JCPDS:79-0207). According to JCPDS data (76-1730), the distinct diffraction peaks at $2\theta = 24.98$, 26.23 , 27.94 , 33.00 , 37.70 and 39.75° can be well indexed to the monoclinic phase of crystalline $\alpha\text{-Bi}_2\text{O}_3$ (102), (002), (012), (121), (112) and (131) crystal planes of Bi_2O_3 [16]. The peak located at 30.46 can be indexed to (222) planes of cubic Bi_2O_3 standard card 00-006-0312. In the case of $\text{ZnBi}_2\text{O}_4/\text{rGO}$ materials, almost all of the diffraction peaks exhibited similar to those of the pristine ZnBi_2O_4 ; however, some new peaks had been identified at $2\theta = 27.15$, 28.10 , 29.70 and 37.10° that may be due to the formation of heterojunction between rGO and ZnBi_2O_4 . The sharp and symmetrical diffraction peaks indicate the high degree crystallinity of the sample.

Figure 1b shows the UV-vis diffuse reflectance spectra (DRS) of pristine rGO, pristine ZnBi_2O_4 and $\text{ZnBi}_2\text{O}_4/\text{rGO}$ samples. The absorbance of the pristine rGO sample extended from visible to infrared region. In case of pristine ZnBi_2O_4 , the absorbance of the sample extended into visible light region, indicating that this material is visible-light responsive, and therefore this material is capable of being a photocatalyst under visible light irradiation. However, the presence of rGO in the $\text{ZnBi}_2\text{O}_4/\text{rGO}$ has caused the expansion of the visible light absorbing region. All of the UV-vis absorption edges of $\text{ZnBi}_2\text{O}_4/\text{rGO}$ samples appeared at 455 nm, showing redshift compared to that of the pristine ZnBi_2O_4 (UV-vis absorption edge at 435 nm). This change is attributed to the chemical bonding between rGO and ZnBi_2O_4 in the $\text{ZnBi}_2\text{O}_4/\text{rGO}$ photocatalysts, probably due to the formation of Zn-C and Bi-C bonds in $\text{ZnBi}_2\text{O}_4/\text{rGO}$ [17,18]. These results show that $\text{ZnBi}_2\text{O}_4/\text{rGO}$ is a promising catalyst under visible light irradiation.

The FT-IR spectra of pristine rGO, ZnBi_2O_4 and $\text{ZnBi}_2\text{O}_4/\text{rGO}$ samples are shown in Figure 1c. FT-IR spectrum of pristine ZnBi_2O_4 has shown characteristic vibrational peaks of Bi-O and Bi-O-Bi stretching modes at 1391 cm^{-1} and 843 cm^{-1} , respectively. The peak observed at 485 cm^{-1} of ZnBi_2O_4 spectrum is ascribed to Zn-O stretching. In case of rGO, typical bands at 1721 cm^{-1} and 1222 cm^{-1} are attributed to C=O and C-OH stretching modes, respectively [19]. The peak at 1577 cm^{-1} in rGO spectrum is attributed to the ring skeletal vibration [20]. The spectrum of $\text{ZnBi}_2\text{O}_4/\text{rGO}$ samples exhibit characteristic peaks similar to pristine ZnBi_2O_4 ; however, characteristic vibrational peaks of rGO cannot be seen clearly.

In order to further investigate the structural characteristics and the interfacial features of as-prepared samples, FE-SEM and TEM image of materials were conducted and is presented in Figure 2. The FE-SEM micrographs revealed that the rGO sample was piled up to a sheet-shape while the image of ZnBi_2O_4 showed irregular stacking particles (Figure 2a). From the FE-SEM and TEM images of samples, it was found that the rGO were densely covered by the ZnBi_2O_4 plates.

3.2. Photocatalytic activity

The photocatalytic activities of the as-prepared catalysts were evaluated by measuring the degradation of Indigo carmine under visible light and present in Figure 3a. Before irradiation, the dark adsorption equilibrium was established for 30 min. As seen in Figure 3a, the Indigo

carmine was degraded by approximately 10 % within 75 min of visible light exposure without a catalyst, indicating that photolysis contributes to the degradation of Indigo carmine.

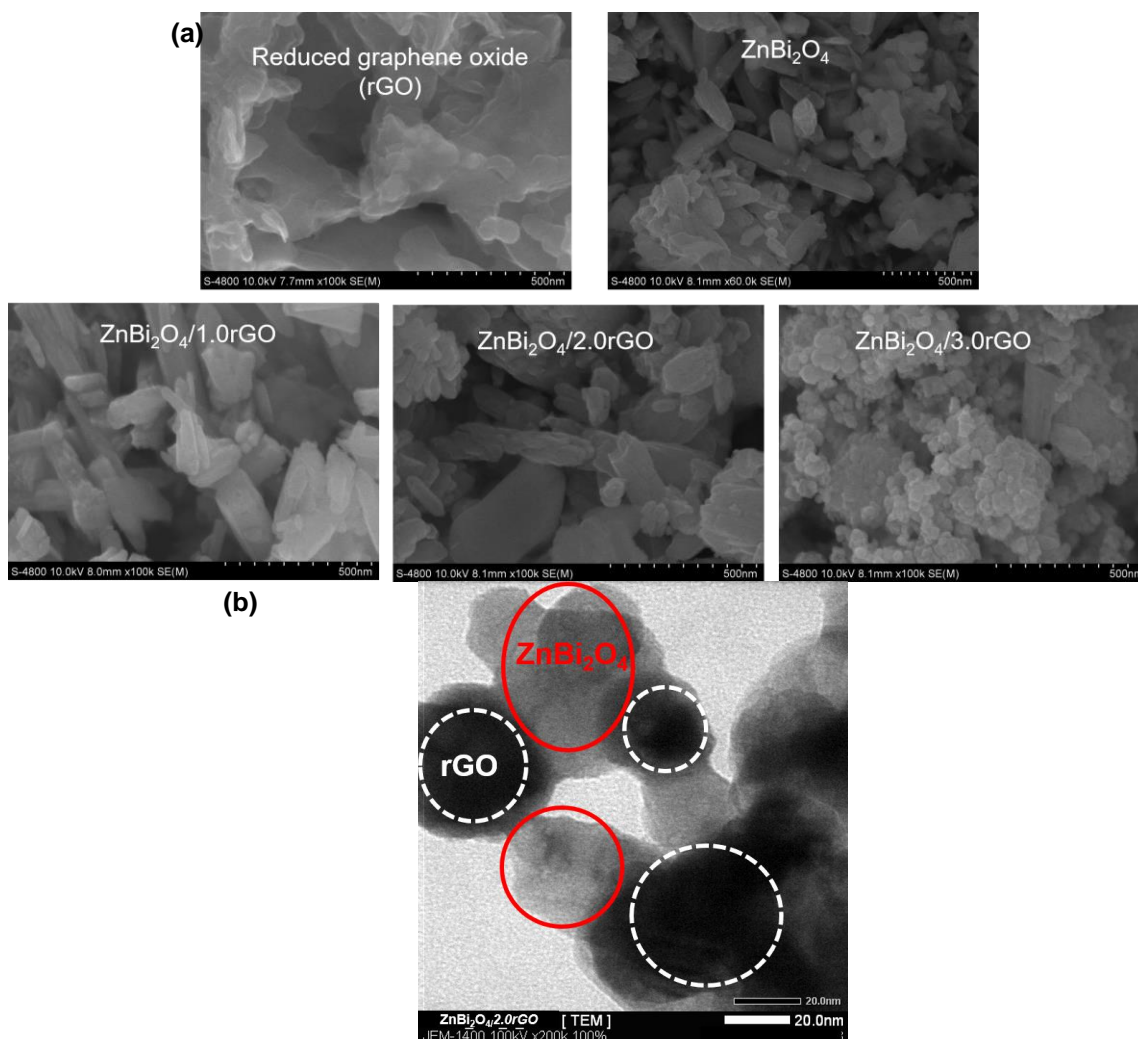


Figure 2. (a) FE-SEM and (b) TEM image of as-prepared samples.

The degradation of Indigo carmine was accelerated in the presence of catalysts. Under visible light, approximately 34 % Indigo carmine was degraded by introducing pristine ZnBi₂O₄ catalyst. As seen in Figure 3a, it is evident that the ZnBi₂O₄ loading on rGO significantly enhances the photocatalytic activity of ZnBi₂O₄/rGO hybrid catalysts. The ZnBi₂O₄/2.0rGO catalyst had excellent photocatalytic activity; more than 91 % of Indigo carmine (50 mg/L) degraded during 75 min in visible light. Approximately 57 % and 64 % of Indigo carmine has been degraded within 75 min using ZnBi₂O₄/1.0rGO and ZnBi₂O₄/3.0rGO, respectively. This result indicated that the photogenerated charges carriers in ZnBi₂O₄/1.0rGO catalyst is insufficient to produce the active species. However, the excessive rGO in ZnBi₂O₄/3.0rGO catalyst may act as mediators for the recombination of photoinduced e^- and h^+ , ultimately reducing the photocatalytic activity [4]. It is obvious that the optimal rGO loading amount significantly affects the photocatalytic activity of ZnBi₂O₄/rGO binary catalysts.

Few studies have reported the Indigo carmine degradation using different catalysts. It has been reported that complete degradation of Indigo carmine occurs over TiO_2/UV , photo-fenton oxidation and $\text{Nd-TiO}_2\text{-GO/Vis}$ systems [1,21]. The degradation of Indigo carmine using CdS/blue LED system has been tested. The results showed that approximately 80 % of 10 mg/L of Indigo carmine was degraded after 0.08 h of irradiation [3]. The catalytic degradation in a Eu,C,N,S-ZrO_2 (0.6 % Eu)/visible light achieved almost 100 % of 20 mg/L of Indigo carmine was degraded after 150 min of irradiation [22]. The photocatalytic degradation of 0.05-0.4 mM Indigo carmine in a TiO_2 impregnated activated carbon ($\text{TiO}_2\text{:AC}$)/UV system achieved 70.69 - 91.06 % after 4 h of irradiation [23].

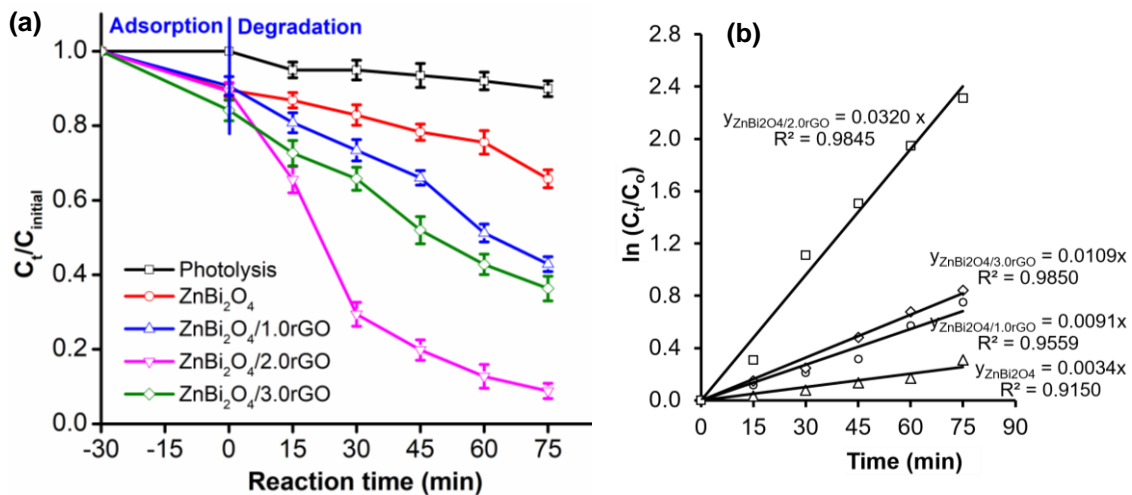


Figure 3. (a) Photodegradation and (b) Linear kinetic degradation of Indigo carmine using $\text{ZnBi}_2\text{O}_4/\text{rGO}$ catalysts under visible light irradiation.

First-order kinetics were used to analyze the experimental kinetic data, which can be expressed as $\ln(C_0/C_t) = kt$, where t is the reaction time (min), k is the apparent rate constant (min^{-1}), and C_0 and C_t are the Indigo carmine concentrations (mg/L) at times of $t = 0$ and $t = t$, respectively. Plotting $\ln(C_0/C_t)$ versus reaction time, t , yields a straight line, where the slope is the apparent rate constant. The rate constants for the catalysis are included in Figure 3b. The kinetic data for Indigo carmine degradation were consistent with pseudo-first-order kinetics ($r^2 = 0.9150 - 0.9850$). The order of the Indigo carmine degradation rates for the photocatalysts is $\text{ZnBi}_2\text{O}_4/2.0\text{rGO}$ ($k = 0.0320 \text{ min}^{-1}$) > $\text{ZnBi}_2\text{O}_4/3.0\text{rGO}$ ($k = 0.0109 \text{ min}^{-1}$) > $\text{ZnBi}_2\text{O}_4/1.0\text{rGO}$ ($k = 0.0091 \text{ min}^{-1}$) > pristine ZnBi_2O_4 ($k = 0.0034 \text{ min}^{-1}$). The $\text{ZnBi}_2\text{O}_4/2.0\text{rGO}$ catalyst exhibited the highest visible light photocatalytic activity for Indigo carmine degradation. The photodegradation rates of Indigo carmine over $\text{ZnBi}_2\text{O}_4/\text{rGO}$ catalysts were between 2.7 to 9.4 times higher than that of pristine ZnBi_2O_4 . Thus, the hybridization of ZnBi_2O_4 with rGO greatly enhances the rate of Indigo carmine oxidation.

The effect of $\text{ZnBi}_2\text{O}_4/2.0\text{rGO}$ dosage on the photocatalytic degradation of Indigo carmine was studied by varying the amount of catalyst from 0.2 to 2.0 g/L at the optimal condition: 50 mg/L Indigo carmine, pH = 6.3. As seen in Figure 4b, increasing the amount of $\text{ZnBi}_2\text{O}_4/2.0\text{rGO}$ catalyst from 0.2 to 1.0 g/L leads to an increase in the percent degradation, this may be attributed to the increased generation of reactive radicals from the $\text{ZnBi}_2\text{O}_4/2.0\text{rGO}$ surface when increasing the catalyst amount. For 1.0 g/L $\text{ZnBi}_2\text{O}_4/2.0\text{rGO}$ catalyst, 91% of Indigo carmine

was degraded after 75 min. However, the amount of $\text{ZnBi}_2\text{O}_4/2.0\text{rGO}$ was more than 1.0 g/L, leading to decrease Indigo carmine degradation, which may be due to the excessive catalyst causing opacity of the solution, thereby hindering the light penetration into the suspension and consequently interfering with the Indigo carmine degradation reaction.

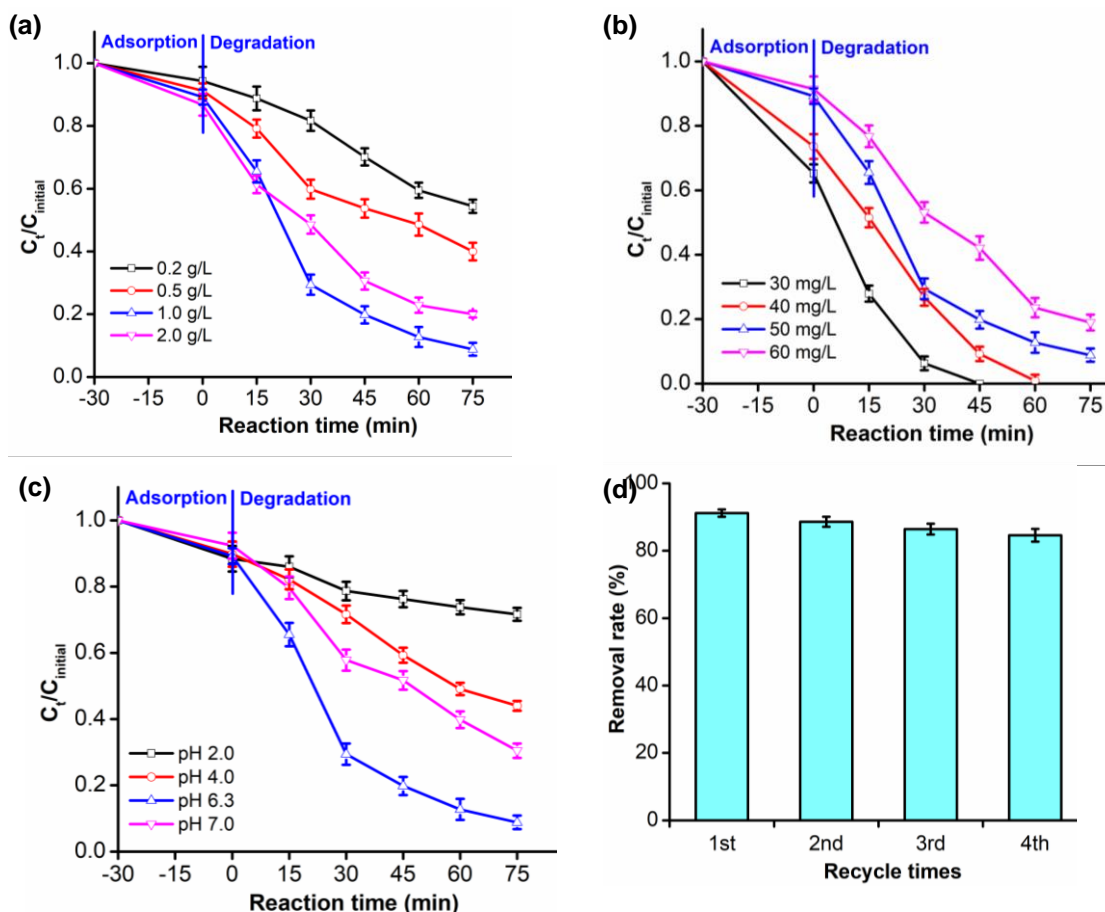


Figure 4. (a) Effect of $\text{ZnBi}_2\text{O}_4/2.0\text{rGO}$ amount; (b) Effect of initial Indigo carmine concentration; (c) Effect of pH solution and (d) Reusability of $\text{ZnBi}_2\text{O}_4/2.0\text{rGO}$ hybrid catalyst.

The effect of initial Indigo carmine concentration on the photocatalytic degradation process was obtained by varying the Indigo carmine concentration from 30 to 60 mg/L at the optimal condition: $\text{ZnBi}_2\text{O}_4/2.0\text{rGO}$ catalyst = 1.0 g/L, pH = 6.3 (Figure 4b). The catalytic degradation decreases with increasing of Indigo carmine concentration. This is explainable by the fact that when the amount of catalyst is maintained constant (at 1.0 g/L), the number of reactive radicals is also unchanged, while the initial concentration of Indigo carmine is increased, so the ratio between number of reactive radicals to Indigo carmine molecules decreases, therefore the complete Indigo carmine degradation requires a longer time. Hence, 50 mg/L is the optimal Indigo carmine concentration for degradation.

It is well-known the efficiency of photocatalytic degradation process strongly depends on pH of the reaction solution. The effect of pH on the photocatalytic degradation process was studied by varying pH from 2.0 to 7.0 using a few drops of 0.1 M HCl or NaOH at the optimal

condition: $\text{ZnBi}_2\text{O}_4/2.0\text{rGO}$ catalyst = 1.0 g/L, Indigo carmine concentration = 50 mg/L. Figure 4c shows that the maximum degradation of 50 mg/L of Indigo carmine over $\text{ZnBi}_2\text{O}_4/2.0\text{rGO}$ catalyst was more than 91% for a duration of 75 min at pH 6.3, while 28%, 56% and 67% of Indigo carmine was degraded at pH 2.0, 4.0 and 7.0, respectively.

The reusability of catalysts is important to assess the potential of applications in water and wastewater treatment. Therefore, the recycling of $\text{ZnBi}_2\text{O}_4/2.0\text{rGO}$ catalyst was evaluated by degradation of Indigo carmine over four consecutive cycles under visible light. Experiments on the reusability of catalyst were carried out at the optimal condition: $\text{ZnBi}_2\text{O}_4/2.0\text{rGO}$ catalyst = 1.0 g/L, Indigo carmine concentration = 50 mg/L and pH = 6.3. After visible-light irradiation for 75 min, the solution was discolored. The catalyst was separated by centrifugation and then the dried catalyst was used again for subsequent experiment. As shown in Figure 4d, $\text{ZnBi}_2\text{O}_4/2.0\text{rGO}$ exhibited high photochemical stability, even though the photocatalyst had been recycled four times successively. This implied that the progressive reduction after fourth consecutive cycles was very small. Approximately 84.60% of Indigo carmine had been successfully degraded after four runs, indicating that the loss in photocatalytic performance of $\text{ZnBi}_2\text{O}_4/2.0\text{rGO}$ was insignificant after four recycling runs.

The mineralization of Indigo carmine over $\text{ZnBi}_2\text{O}_4/2.0\text{rGO}$ catalyst was clarified by determining the total organic carbon (TOC) in the reaction solution at the optimal condition: $\text{ZnBi}_2\text{O}_4/2.0\text{rGO}$ catalyst = 1.0 g/L, Indigo carmine concentration = 50 mg/L and pH = 6.3. It can be found that the TOC removal efficiency is approximately 79.6 % after 75 min of photocatalytic reaction under visible light, which confirmed the outstanding mineralization performance of $\text{ZnBi}_2\text{O}_4/2.0\text{rGO}$ binary catalyst. The $\text{Fe}^{2+}/\text{UV}/\text{H}_2\text{O}_2$ system mineralized about 42% of Indigo carmine 20 mg/L at pH 5.6 in the presence of 69.9 mg/L of H_2O_2 and 5 mg/L Fe^{2+} after 30 min of visible light irradiation [1]. The mineralization of Indigo carmine (20 mg/L) in TiO_2/UV light system achieved about 23% after 60 minutes of irradiation [1].

3.3. Trapping experiment

In order to understand more about the mechanism of the enhanced photocatalytic activity of $\text{ZnBi}_2\text{O}_4/2.0\text{rGO}$ catalyst, three scavengers were used to identify the active species in the photocatalytic process. *Tert*-butanol ($\text{C}_9\text{H}_{10}\text{O}$, 2 mmol/L) as a $\text{OH}\cdot$ radical scavenger, *p*-benzoquinone ($\text{C}_6\text{H}_4\text{O}_2$, 2 mmol/L) as a superoxide anion radical scavenger, disodium ethylenediamine tetraacetate ($\text{Na}_2\text{-EDTA}$, 1 mmol/L) as a hole scavenger, were added to the solution. As shown in Figure 5a, the photodegradation of RhB was apparently decreased after the injection of *p*-benzoquinone (a scavenger of $\text{O}_2^{\cdot-}$). Indeed, in the presence of *p*-benzoquinone, only 23% of Indigo carmine was degraded after 75 min. The rate constant (k) was reduced from 0.0320 min^{-1} to 0.0020 min^{-1} (decreased 16 fold). (Figure 5b). The addition of $\text{Na}_2\text{-EDTA}$ caused a small change in the photocatalytic degradation of Indigo carmine, and approximately 58% of Indigo carmine photodegradation took place. Thus, the k value was decreased from 0.0320 min^{-1} to 0.0110 min^{-1} in the absence of photoinduced h^+ (decreased 2.9 fold). In contrast, the addition of *tert*-butanol had a little effect on the degradation rate of Indigo carmine, the rate constant (k) was reduced from 0.0320 min^{-1} to 0.0153 min^{-1} when $\text{OH}\cdot$ radical was removed. These results indicate that $\text{O}_2^{\cdot-}$ is the major active species responsible for the complete photocatalytic mineralization of Indigo carmine, whereas the contribution of the photoinduced h^+ and $\text{OH}\cdot$ radicals are assistant active species.

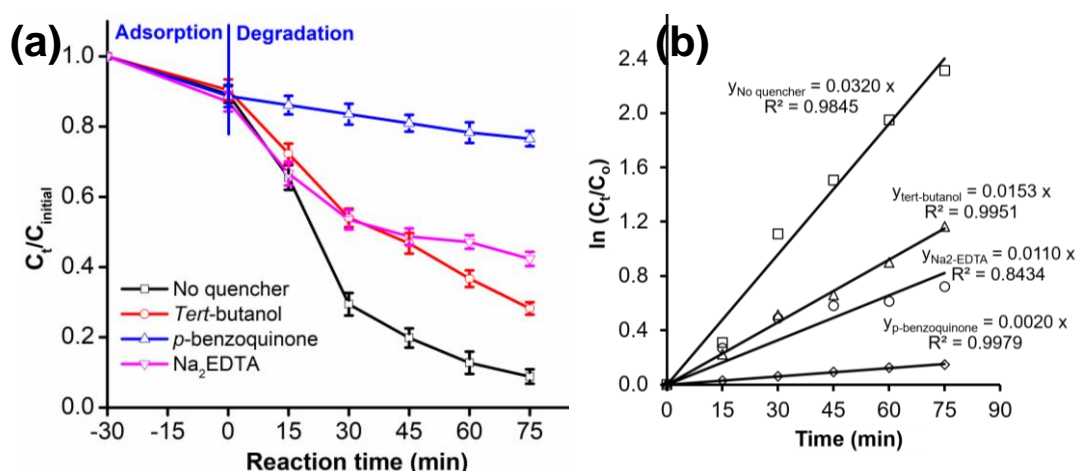


Figure 5. (a) Photodegradation and (b) Linear kinetic degradation of Indigo carmine using ZnBi₂O₄/2.0rGO under visible light with addition of photoinduced h^+ ; O₂^{•-} and OH[•] radical scavengers.

3.4. Photocurrent analysis and proposed photodegradation mechanism

In order to provide more evidence of photoinduced electron and hole separation, a transient photocurrent response analysis was performed under visible light irradiation. Presently, the photocurrent is widely regarded as the most efficient separation of photoinduced $e^- - h^+$ pairs in the composite photocatalysts [24]. Photocurrent measurements were performed in the three electrode photoelectrochemical system. Solution 0.5 M Na₂SO₄, a platinum wire and a Ag/AgCl electrode was used as an electrolyte, the counter electrode and the reference electrode, respectively.

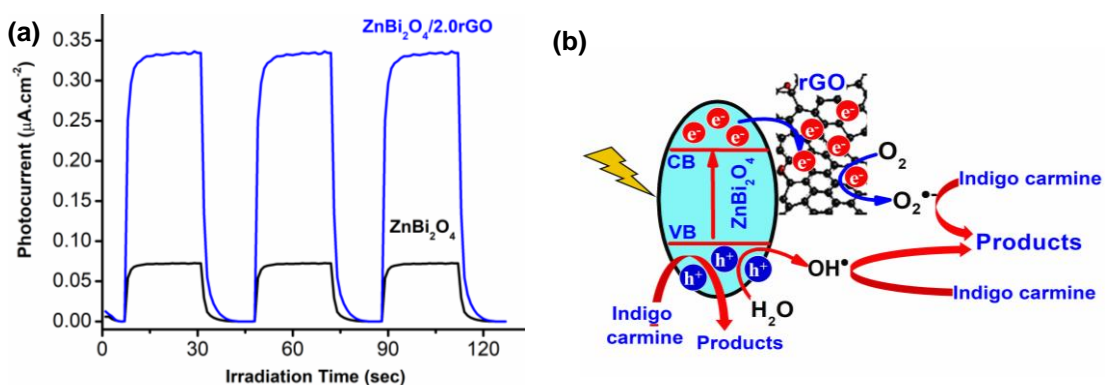


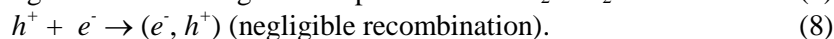
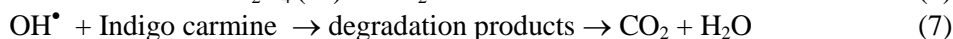
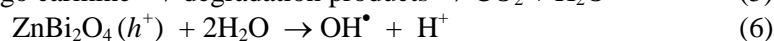
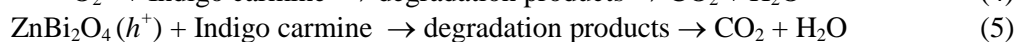
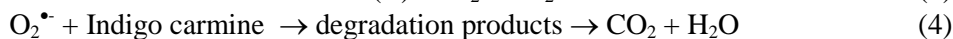
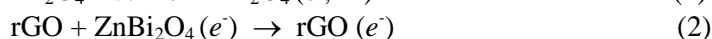
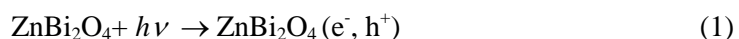
Figure 6. (a) Photocurrent response for ZnBi₂O₄ and ZnBi₂O₄/2.0rGO samples and (b) Proposed photodegradation mechanisms of Indigo carmine using ZnBi₂O₄/2.0rGO.

Figure 6a shows the ZnBi₂O₄/2.0rGO binary sample presents the quite high photocurrent intensity, which is about five times higher than that of pristine ZnBi₂O₄. This indicated that rGO acts as photoinduced e^- acceptor from ZnBi₂O₄, so that the lifetime of the photoinduced e^- in the ZnBi₂O₄/2.0rGO sample is longer than that of pristine ZnBi₂O₄. A higher photocurrent response value indicates the lower photoinduced $e^- - h^+$ pairs recombination rate, and thus, the higher the

photocatalytic activity. The result of photocurrent analysis is consistent with the photocatalytic testing results.

Based on the analysis and characterization of the experimental results above, the proposed mechanism of the Indigo carmine degradation over ZnBi₂O₄/2.0rGO hybrid catalyst under visible light is shown in Figure 6b. Under visible light, ZnBi₂O₄ in the hybrid catalyst could be excited and produced large numbers of photoinduced e^- - h^+ pairs. As soon as the photoinduced e^- of the ZnBi₂O₄ were generated, they could directly move into the rGO through its alternate conjugation. The photoinduced e^- and h^+ could react with oxygen and H₂O molecules adsorbed onto ZnBi₂O₄/2.0rGO surface to form O₂^{•-} and OH[•] radicals, respectively. The formed O₂^{•-} and OH[•] radicals and photoinduced h^+ could efficiently degrade Indigo carmine into CO₂ and water. Due to charge transportation, the rGO in ZnBi₂O₄/2.0rGO could serve as a photoinduced e^- acceptor.

The photodegradation mechanism of Indigo carmine by the ZnBi₂O₄/2.0rGO catalyst can be described by the following reactions:



4. CONCLUSIONS

A series of ZnBi₂O₄/rGO hybrid catalysts with high visible light photocatalytic activity were successfully prepared via co-precipitation method. The ZnBi₂O₄/2.0rGO catalyst displayed excellent photocatalytic activity as well as stability for degradation of Indigo carmine at least in four consecutive experiments under visible light. The rGO acted as good electron acceptor and thus inhibited the photoinduced e^- and h^+ recombination, consequently, enhanced the degradation activity of the ZnBi₂O₄/2.0rGO hybrid catalyst. A study to identify active species indicated that O₂^{•-} radicals was the main active species in the Indigo carmine degradation process while photoinduced h^+ and OH[•] radicals contributed as active assistants. This study highlights that the ZnBi₂O₄/2.0rGO hybrid catalyst is a promising semiconductor photocatalyst candidate for environmental remediation under visible light.

Acknowledgements: This research is funded by Vietnam National Foundation for Science and Technology Development (NAFOSTED) under grant number 104.05-2017.29.

REFERENCES

1. Ricardo E. Palma-Goyes, Javier Silva-Agredo, Ignacio González, Ricardo A. Torres-Palma -Comparative degradation of indigo carmine by electrochemical oxidation and advanced oxidation processes, *Electrochimica Acta* **140** (2014) 427-433.

2. Salah Ammar, Ridha Abdelhédi, Cristina Flox, Conchita Arias, E. Brillas - Electrochemical degradation of the dye indigo carmine at boron-doped diamond anode for wastewater remediation, *Environmental Chemistry Letters* **4** (4) (2006) 229-233.
3. Agileo Hernández-Gordillo, Vicente Rodríguez-González, Socorro Oros-Ruiz, Ricardo Gómez - Photodegradation of Indigo Carmine dye by CdS nanostructures under blue-light irradiation emitted by LEDs, *Catalysis Today* **266** (2016) 27-35.
4. Bui The Huy, Chu Thi Bich Thao, Van Duong Dao, Nguyen Thi Kim Phuong, Yong-III Lee - A Mixed-Metal Oxides/Graphitic Carbon Nitride: High Visible Light Photocatalytic Activity for Efficient Mineralization of Rhodamine B, *Advanced Materials Interfaces* **4** (12) (2017) 1700128.
5. Yunjin Yao, Jiacheng Qin, Yunmu Cai, Fengyu Wei, Fang Lu, Shaobin Wang - Facile synthesis of magnetic ZnFe₂O₄-reduced graphene oxide hybrid and its photo-Fenton-like behavior under visible irradiation, *Environmental Science and Pollution Research* **21** (2014) 7296-7306.
6. Leticia M. Torres-Martinez, Miguel A. Ruiz-Gomez, M.Z. Figueroa-Torres, Isaias Juarez-Ramirez, Edgar Moctezuma - Sm₂FeTaO₇ Photocatalyst for Degradation of Indigo Carmine Dye under Solar Light Irradiation, *International Journal of Photoenergy* **1-7** (2012) 939608.
7. Shuang Zhong, Fengjun Zhang, Wei Lu, Tianye Wang, Liyuan Qu - One-step synthesis of Bi₂WO₆/Bi₂O₃ loaded reduced graphene oxide multicomponent composite with enhanced visible-light photocatalytic activity, *RSC Advances* **5** (2015) 68646-68654.
8. Hong Liu, Zhitong Jin, Yun Su, Yong Wang - Visible light-driven Bi₂Sn₂O₇/reduced graphene oxide nanocomposite for efficient photocatalytic degradation of organic contaminants, *Separation and Purification Technology* **142** (2015) 25-32.
9. Martinez-de La Cruz A., Obregón Alfaro S. - Synthesis and characterization of γ -Bi₂MoO₆ prepared by co-precipitation: photoassisted degradation of organic dyes under vis-irradiation, *Journal of Molecular Catalysis A: Chemical* **320** (1-2) (2010) 85-91.
10. Jiwen Zhang, Yanyan Jiang, Wenyuan Gao, Hongshun Hao - Synthesis and visible photocatalytic activity of new photocatalyst MBi₂O₄(M = Cu, Zn), *Journal of Materials Science: Materials in Electronics* **26** (2015) 1866-1873.
11. Karan Goswamia, Rajakumar Ananthkrishnana - Facile synthesis of nano Zn/Bi - reduced graphene oxide for enhanced photocatalytic elimination of chlorinated organic pollutants under visible light. *New Journal of Chemistry* **41** (2017) 4406-4415.
12. Virendra Singh, Daeha Joung, Lei Zhai, Soumen Das, Saiful I. Khondaker, Sudipta Seal - Graphene based materials: Past, present and future, *Progress in Materials Science* **56** (2011) 1178-1271.
13. El-Khodary S.A., El-Enany G.M., El-Okr M., Ibrahim M. - Preparation and characterization of microwave reduced graphite oxide for high-performance supercapacitors, *Electrochimica Acta* **150** (2014) 269-278.
14. William S. Hummers Jr., Richard E. Offeman - Preparation of Graphitic Oxide, *Journal of the American Chemical Society* **80** (6) (1958) 1339-1339.
15. Songfeng Pei, Jinping Zhao, Jinhong Du, Wencai Ren, Hui-Ming Cheng - Direct reduction of graphene oxide films into highly conductive and flexible graphene films by hydrohalic acids, *Carbon* **48** (15) (2010) 4466-4474.

16. Jabeen Fatima M. J, Niveditha C. V and Sindhu S. - α - Bi_2O_3 photoanode in DSSC and study of the electrode–electrolyte interface, *RSC Advances* **5** (2015) 78299-78305
17. Xinjuan Liu, Likun Pan, Tian Lv, Ting Lu, Guang Zhu, Zhuo Sun, Changqing Sun - Microwave Assisted Synthesis of ZnO-Graphene Composite for Photocatalytic Reduction of Cr(VI), *Catalysis Science & Technology* **1** (7) (2011) 1189- 1193.
18. Yinzhou Wang, Wei Wang, Hongying Mao, Yunhao Lu, Jianguo Lu, Jingyun Huang, Zhizhen Ye, Bin Lu. - Electrostatic Self-Assembly of BiVO_4 -Reduced Graphene Oxide Nanocomposites for Highly Efficient Visible Light Photocatalytic Activities, *ACS Applied Materials & Interfaces* **6** (15) (2014) 12698-12706.
19. Nan Wu, Xilin She, Dongjiang Yang, Xiaofeng Wu, Fabing Su, Yunfa Chen - Synthesis of network reduced graphene oxide in polystyrene matrix by a two-step reduction method for superior conductivity of the composite, *Journal of Materials Chemistry* **22** (33) (2012) 17254-17261.
20. Bihe Yuan, Lei Song, Kim Meow Liew, Yuan Hu - Solid acid-reduced graphene oxide nanohybrid for enhancing thermal stability, mechanical property and flame retardancy of polypropylene, *RSC Advances* **5** (51) (2105) 41307-41316.
21. Samuel Osei-Bonsu Oppong, William W. Anku, Sudheesh K. Shukla, Eric S. Agorku, Poomani P. Govender - Photocatalytic degradation of indigo carmine using Nd-doped TiO_2 -decorated graphene oxide nanocomposites, *Journal of Sol-Gel Science and Technology* **80** (1) (2016) 38–49.
22. Agorku E.S., Kuvarega A.T., Mamba B.B., Pandey A.C., Mishra A.K. - Enhanced visible-light photocatalytic activity of multi-elements-doped ZrO_2 for degradation of indigo carmine, *Journal of Rare Earths* **33** (5) (2015) 498-506.
23. Subramani A. K., Byrappa K., Ananda S., Lokanatha Rai K. M., Ranganathaiah C., Yoshimura M. - Photocatalytic degradation of indigo carmine dye using TiO_2 impregnated activated carbon, *Bulletin of Materials Science* **30** (1) (2007) 37-41.
24. Li T., Zhao L., He Y., Cai J., Luo M., Lin J. - Synthesis of g- $\text{C}_3\text{N}_4/\text{SmVO}_4$ composite photocatalyst with improved visible light photocatalytic activities in RhB degradation, *Applied Catalysis B: Environmental* **129** (2013) 255-263.